Inorg. Chem. **1990**, *29*, 2842–2847

Contribution from the Department of Chemistry,
State University of New York at Buffalo, Buffalo, New York 14214

Oxide and Hydroxide Species Formed on Addition of Water in Ambient-Temperature Chloroaluminate Melts: An ^{17}O NMR Study

Thomas A. Zawodzinski, Jr.,[†] and R. A. Osteryoung*

Received November 7, 1989

The variation of the intensity of ^{17}O NMR lines with manipulation of proton concentration and melt composition has been used to model oxy- and hydroxychloroaluminate species in the ambient-temperature molten salt system 1-ethyl-3-methylimidazolium chloride/aluminum chloride. It is concluded that the most probable oxychloroaluminate species in acidic melts are $Al_3OCl_8^-$ and either $Al_3O_2Cl_6^-$ or $Al_2OCl_5^-$ and the most probable hydroxychloroaluminate species are $Al_3Cl_9OH^-$ and $Al_2Cl_6OH^-$, with the latter being favored. In the basic melts, the most probable oxy- and hydroxychloroaluminate species are $Al_2OCl_5^-$ and $Al_2Cl_6OH^-$.

Introduction

The chemistry of water in chloroaluminate melts has been examined by using a wide range of techniques for both "high-temperature" molten salts (e.g. $NaCl/AlCl_3$ melts) and ambient-temperature systems.[1-10] Water is of importance in the chemistry of chloroaluminate melts because of its ubiquitous presence as an impurity. Many cases of interactions of solutes with oxide and/or protons present in chloroaluminate melts, which arise from aqueous impurities, have been reported,[2,3,9] and it is likely that these played an unsuspected role in some chemical systems studied in early work with the ambient-temperature chloroaluminates.

Methods of removing both oxide and protons from ambient-temperature chloroaluminates have recently been reported,[10-12] and thus water can be removed from the melts. Nevertheless, an overall description of the chemistry of water and oxide in this class of melts is lacking and is attempted in this report.

We have previously used ^{17}O NMR to study the chemistry of water in ambient-temperature chloroaluminate melts consisting of mixtures of 1-ethyl-3-methylimidazolium chloride (ImCl) with $AlCl_3$ in various mole ratios.[6] In acidic melts, which contain $AlCl_3$ in molar excess, three separate ^{17}O resonance peaks were observed, corresponding to three distinct oxygen-bearing species. The positions of these peaks were independent of melt composition and water concentration; however the relative intensities of the lines varied with these factors. One of the peaks was shown to correspond to oxygen in a hydroxychloroaluminate complex, while the remaining peaks were for oxygens in oxychloroaluminate complexes. In basic melts, a single ^{17}O peak was observed. The position of this peak changed only slightly with changes in melt composition. Upon addition of HCl, the peak shifted markedly upfield. These observations were interpreted as indicating the existence of rapid exchange between two or more oxy- and hydroxychloroaluminate environments.

An important recent contribution to the study of water chemistry in these melts has resulted from mass spectrometric studies.[7,8] Assignment of peaks observed in these studies to specific oxy- and hydroxychloroaluminate species was possible. In the initial study, three dominant species containing oxygen atoms in acidic melts were observed by using SIMS. In a more recent study,[8] a larger number of species containing oxygen atoms was observed by FAB-MS, a SIMS technique. Only $Al_2OCl_5^-$ was observed[8] in the latter study in basic melts, while oxide- or hydroxide-containing species were observed in basic melts in the former study.

Unfortunately, it is difficult, from the work presented in these papers, to draw firm conclusions concerning the actual solution species that result from the addition of water to the chloroaluminate melts, let alone the amount of each present. Little is known about the fragmentation of species liberated from the melt. In acidic melts, considerable evaporation of $AlCl_3$ from the surface of the drop of the melt occurs.[7] Thus the melt composition from which species are evolved is ill-defined. The water itself was, in fact, introduced to the melt in an adventitious manner during sample transfer. These difficulties preclude straightforward identification of the solution species actually formed by water in the melt.

The ^{17}O results presented in our previous work provided a qualitative indication of speciation in the melt. Since then, we have reported on reagents that allow us to quantitatively add protons[13] to or, as noted above, remove protons[12] from the melts. With the tools available to manipulate the proton chemistry in the melt, a more detailed elucidation of the chemistry of oxide and water in the melt is now possible. Our previous study suggested that it is feasible to obtain quantitative information from ^{17}O integrated intensities.

In the present work, the variation in intensity of the ^{17}O spectral lines with proton concentration and melt composition is modeled to obtain possible stoichiometries of the oxy- and hydroxychloroaluminate species in acidic melts and the equilibrium constants for equilibria among these species. In addition, further observations on the behavior of water in basic melts are reported.

Experimental Section

The general procedure for preparation of melt components and melts was as described elsewhere.[14] Careful preparation of ImCl under rigorously anhydrous conditions is necessary to ensure a low initial level of impurities in the melts. The synthesis of ImCl consists of the reaction of 1-methylimidazole with ethyl chloride in a pressure vessel. Several improvements in the purification of starting materials and in handling and workup of the ImCl salt have been implemented. All handling of materials during reagent purification, loading of the reaction vessel, or workup of the product was carried out in Schlenkware under nitrogen or in a drybox. Ethyl chloride was distilled from P_2O_5, while 1-methylimidazole was stirred over KOH and distilled one or more times under reduced pressure to yield a colorless liquid. Workup of the ImCl product consisted of recrystallization from acetonitrile, with ethyl acetate added to force the salt out of solution. After several recrystallizations, the white solid product was heated to about 110 °C and the molten ImCl pumped on for several hours. This final step is carried out to remove traces of ethyl acetate from the salt.

The preparation of $ImHCl_2$ was carried out as previously described.[13] $EtAlCl_2$ was initially used as received (Aldrich Chemical Co.) but, since

(1) Sahami, S.; Osteryoung, R. A. *Anal. Chem.* **1983**, *55*, 1970.
(2) Stojek, Z.; Linga, H.; Osteryoung, R. A. *J. Electroanal. Chem. Interfacial Electrochem.* **1981**, *119*, 365.
(3) Linga, H.; Stojek, Z.; Osteryoung, R. A. *J. Am. Chem. Soc.* **1981**, *103*, 3754.
(4) Berg, R.; Hjuler, H. A.; Bjerrum, N. J. *Inorg. Chem.* **1984**, *23*, 557.
(5) Zachariassen, K.; Berg, R.; Bjerrum, N. J.; von Barner, J. H. *J. Electrochem. Soc.* **1987**, *134*, 1153.
(6) Zawodzinski, T. A.; Osteryoung, R. A. *Inorg. Chem.* **1987**, *26*, 2920.
(7) Franzen, G.; Gilbert, B. P.; Pelzer, G.; DePauw, E. *Org. Mass Spectrom.* **1986**, *21*, 443.
(8) Wicelinski, S. P.; Gale, R. J.; Pamidi, K. M.; Laine, R. A. *Anal. Chem.* **1988**, *60*, 2228.
(9) Carlin, R. T.; Osteryoung, R. A. *Inorg. Chem.* **1988**, *27*, 1482.
(10) Abdul-Sada, A. K.; Avent, A. G.; Parkington, M. J.; Ryan, T. A.; Seddon, K. R.; Welton, T. *J. Chem. Soc., Chem. Commun.* **1987**, 1643.
(11) Sun, I-Wen; Ward, E. H.; Hussey, C. L. *Inorg. Chem.* **1987**, *26*, 4309.
(12) Zawodzinski, T. A.; Carlin, R. T.; Osteryoung, R. A. *Anal. Chem.* **1987**, *57*, 2639.
(13) Zawodzinski, T. A.; Osteryoung, R. A. *Inorg. Chem.* **1988**, *27*, 4383.
(14) Zawodzinski, T. A. Ph.D. Thesis, State University of New York, Buffalo, NY, 1989.

[†] Present address: Department MEE-11, MS D429, Los Alamos National Laboratory, Los Alamos, NM 87545.

0020-1669/90/1329-2842\$02.50/0

Table I. ^{17}O Chemical Shifts for Basic Melt Solutions of Water (H^+ Removed)

compn, mole ratio of $AlCl_3$ to ImCl	water concn, mM	chem shift, ppm
0.9	75	68.2
0.8	100	68.2
0.8	75	68.1
0.8	50	68.1
0.8	25	68.2
0.4	100	68.3
0.4	25	68.0

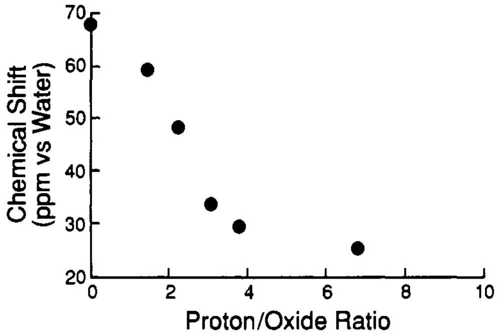

Figure 1. ^{17}O chemical shift of a solution, from which protons were removed, of $H_2{}^{17}O$ in a 0.8:1.0 melt plotted vs the ratio of the proton to oxide concentrations as protons are added back into solution by using $ImHCl_2$.

it became discolored with time, was purified by distillation as necessary. $H_2{}^{17}O$ (20% isotopic enrichment; Cambridge Isotopes) was added to melts with a volumetric pipet.

All NMR samples were prepared in a drybox (Vacuum Atmospheres Co.) operating under a regenerated helium atmosphere. Solutions were pipetted into 10-mm NMR tubes (Wilmad Glass Co.), capped, and sealed with parafilm. All ^{17}O NMR experiments were performed at 90 °C with a JEOL FX-270 NMR spectrometer operating at 36.54 MHz. The NMR experiments are described in more detail in our previous work.[6]

Results and Discussion

1. Basic Melts. Removal of protons is carried out by addition of $EtAlCl_2$, according to the reaction[12]

$$\text{"HCl"} + EtAlCl_2 \rightarrow EtH + AlCl_3 \qquad (1)$$

where "HCl" is the proton-containing species in the melt arising from water addition and may be an –Al–O–H or HCl_2^- species. Removal of protons from solutions of water in basic melts results in a downfield shift of the ^{17}O resonance line observed. When all protons are removed, the peak position is 68.2 ppm, and is independent of concentration and composition of the melt, as summarized in Table I. This strongly suggests that a single oxide species is present in solution in basic melts.

By use of $ImHCl_2$, protons can then be quantitatively added to a melt from which they were removed. Figure 1 shows the ^{17}O chemical shift upon addition of protons, using $ImHCl_2$, to a basic melt solution containing water from which protons were removed.[9,12] The peak shifts downfield as more protons are added. This result is in accord with the previous qualitative conclusions regarding the oxide/hydroxide exchange in water solutions in the basic melts.[6] The concentration of adventitious oxide impurity initially present in these melts is typically a few millimolar.[2,3] A relatively large amount of ^{17}O-labeled water, typically 50–100 mM, was added to the melt in all experiments. Thus, no correction was made to the total oxide present in the melt, and we estimate the error as a maximum of 10% in the total oxide content. This small error in the oxide to proton ratio, though making the data shown in Figure 1 slightly inaccurate on a quantitative basis, does not detract from the qualitative conclusions arrived at on the basis of these data.

Linga et al.[2,3] showed that Ti(IV) dissolved in a basic melt participates in an equilibrium involving oxide dissolved in the melt. Chloro and oxy chloro complexes of Ti(IV) exhibit separate voltammetric waves. When water was added to a solution of Ti(IV) in a basic melt, the wave corresponding to the oxychlorotitanate complex *decreased* in height relative to that of the hexachlorotitanate. Since water is a source of oxide, this result was somewhat surprising. We have employed ^{17}O NMR spectroscopy to investigate this behavior.

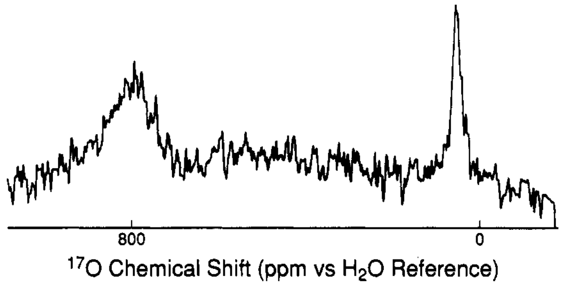

Figure 2. ^{17}O spectrum of a solution of $H_2{}^{17}O$ in a 0.8:1.0 melt with added $TiCl_4$. All protons were removed by addition of $EtAlCl_2$ following $H_2{}^{17}O$ addition.

Table II. ^{17}O Chemical Shifts of Basic Melt Solutions of Water and $TiCl_4$

$[TiCl_4]/[H_2O]$	chem shift ppm Al–O peak	chem shift ppm Ti–O peak	$[TiCl_4]/[H_2O]$	chem shift ppm Al–O peak	chem shift ppm Ti–O peak
0	59.7		1.53	50.3	796
0.87	54.4	781	2.59	45.4	800
1.19	53.7	788			

In Figure 2, an ^{17}O NMR spectrum of a basic melt solution of water to which $TiCl_4$ has been added is shown. Two ^{17}O peaks are seen, and the data obtained from such spectra are summarized in Table II. The peak corresponding to the aluminum–oxy/hydroxy environment shifts upfield as the concentration of Ti(IV) is increased. This result is readily explained by considering the equilibria

$$TiOCl_4^{2-} + 2AlCl_4^- \rightleftarrows TiCl_6^{2-} + Al_2OCl_5^- + Cl^- \qquad (2a)$$

$$Al_2OCl_5^- + HCl \rightleftarrows Al_2Cl_6OH^- \qquad (2b)$$

$$HCl + Cl^- \rightleftarrows HCl_2^- \qquad (2c)$$

$$TiOCl_4^{2-} + 2AlCl_4^- + 2HCl \rightleftarrows TiCl_6^{2-} + Al_2Cl_6OH^- + HCl_2^- \qquad (2d)$$

Increasing the concentration of Ti(IV) results in the "removal" of oxide from the Al–O environment. The proton/Al–O ratio thus increases, and as illustrated by Table II, the Al–O/Al–OH peak observed shifts upfield in accord with the results shown in Figure 1. The broad TiO line (see Figure 2) and the wide spectral window with attendant base-line artifacts precluded the accurate determination of integrated intensities for the two species. This also explains the results obtained by Linga et al.[2,3] upon addition of water to a solution containing Ti(IV) and oxide. Further, if the protons are removed from a solution of $H_2{}^{17}O$ in a basic melt containing Ti(IV), the line observed in the Al–O region of the spectrum is, within experimental error, in the same position as that for a water solution, without Ti(IV), from which protons have been removed, i.e., 68.2 ppm.

2. Oxide Speciation in Acidic Melts. The spectra shown in Figure 3b,c are those resulting from the removal of protons by two successive additions of $EtAlCl_2$ to the solution of water whose spectrum is shown in a. Clearly, species A is the only protonated species of the three, as previously proposed from a totally different, and qualitative, experiment.[6] The summed integrated intensities of the three peaks remain essentially constant as $EtAlCl_2$ is added.

The integrated intensity data for the various peaks as functions of concentration and composition can be modeled by assuming a specific form for each of the oxy- and hydroxychloroaluminate complexes observed and comparing the data obtained experimentally to the behavior predicted for the stoichiometry assumed. In principle, the modeling can be carried out on solutions from

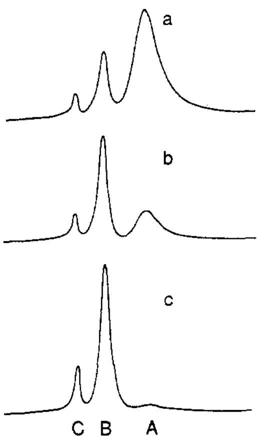

Figure 3. ^{17}O spectra of solutions of $H_2{}^{17}O$ in a 1.2:1.0 melt from which protons are sequentially removed, by using $EtAlCl_2$: (a) 50 mM $H_2{}^{17}O$ solution; (b) 50 mM $H_2{}^{17}O$ + 60 mM $EtAlCl_2$; (c) 50 mM $H_2{}^{17}O$ + 90 mM $EtAlCl_2$. Summed integral intensities (arbitrary units): (a) 333; (b) 332; (c) 327.

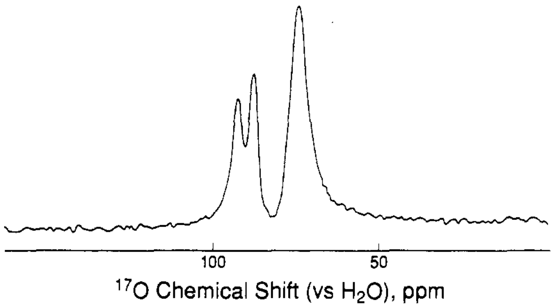

Figure 4. ^{17}O spectrum of a solution of $H_2{}^{17}O$ in a 1.13:1.0 $AlCl_3$/ImCl melt to which more $EtAlCl_2$ than necessary to remove all H^+ has been added (see text).

which protons have been removed quantitatively (for species B and C) and then reconstituted by adding $ImHCl_2$ (for species A).

Unfortunately for us, the straightforward method outlined above has an important limitation in practice. As mentioned above, the addition of water to an acidic melt can result in the evolution of HCl gas upon the initial contact of water with the melt. This leads to problems in obtaining a quantitatively correct model since the loss of HCl results in uncertainty in the actual acidity of the melt, uncertainty in the amount of $EtAlCl_2$ needed to remove protons, and, of course, uncertainty in the proton concentration. An additional factor that compounds the problem is the irreproducibility of the amount of protons lost. Estimates of the amount of protons lost for various experiments range from nearly no loss to a loss of 60% of the protons added with water.

Overtitration of the protons present in the acidic melt with $EtAlCl_2$ resulted in spectra such as shown in Figure 4. Some additional oxygen-containing species must be formed to give rise to the peak at 88 ppm. This peak is probably an oxy chloro complex similar to that which gives rise to peak C, but with an ethyl group substituted for a Cl atom. Interestingly, only a fairly small excess of $EtAlCl_2$, 0.002 01 mol of $EtAlCl_2$ versus 0.001 92 mol of protons nominally present, was added to the melt over that needed to remove the protons resulting from water addition, although the actual excess is somewhat larger since some protons were lost during the dissolution of water, as discussed above. Even so, the $EtAlCl_2$ present in the acidic melt must have a high affinity for oxide; this has not been investigated further. However, if it were assumed that $EtAlCl_2$ behaves like $AlCl_3$, the number of Al atoms present in species B and C could be determined by a careful study of $EtAlCl_2$ in oxide-containing solutions if the spectral line resulting from each species formed by successive additions of $EtAlCl_n$ groups to the aluminum oxy halide species could be resolved. None of the spectra employed in the modeling displayed evidence for the presence of this additional species.

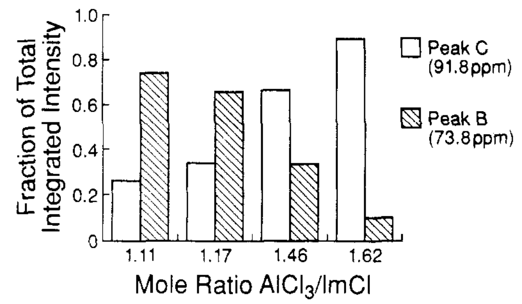

Figure 5. Relative integrated intensities of ^{17}O peaks B and C in acidic melt solutions of $H_2{}^{17}O$, from which protons have been removed, plotted versus melt composition.

Table III. Integrated Intensities and Line Widths Observed for Species B and C by ^{17}O NMR Spectroscopy

melt compn	species B intens[a]	species B fwhh, Hz	species C intens[a]	species C fwhh, Hz	tot. intens
1.20	11.1	174	9.3	119	20.4
1.25	8.4	188	12.5	122	20.9
1.30	8.2	188	12.3	124	20.5
1.32	7.8	193	13.4	124	21.2
1.40	7.4	183	15.3	119	22.7
1.41	7.5	193	14.5	119	22.0
1.47	5.0	179	16.3	119	21.3
1.50	4.7	193	17.4	122	22.1
1.54	3.6	174	19.2	119	22.8
1.60	2.7	197	18.6	119	21.3
					av 21.5 ± 0.8

[a] Integrated intensity given in arbitrary units, corrected for the decay of intensity during predetection delay time.

Typical integrated intensity data for the two oxide species present in an $EtAlCl_2$-treated solution of water in acidic melts of various compositions are shown in Figure 5. Qualitatively, the formation of the species corresponding to peak C is favored by higher $Al_2Cl_7^-$ concentrations, and, conversely, the species corresponding to peak B is favored as the neutral melt region is approached from the acidic side.

The integrated intensities of peaks B and C as functions of composition were determined and were corrected for loss of intensity during the predetection delay time since the line widths differed, and a model, which neglects the loss of HCl but which should be qualitatively correct, was fit to the corrected intensities. The peak intensity data used in the modeling of stoichiometry are shown in Table III, together with the line widths of the lines observed. Note that the sum of the integrated intensities is constant. The determination of the molecular formulas of species B and C, which is mostly dependent on the trend of the relative integrated intensities with composition, should not be strongly affected by errors in the composition, provided that the amounts of HCl lost for the samples used were similar. The experiments were carried out by preparing solutions of $H_2{}^{17}O$ in melts of two different compositions and mixing the solutions to create solutions with intermediate melt compositions. Thus, only two independent HCl concentrations were involved. Hopefully, the loss of HCl was not radically different for the two solutions, prepared in as similar a fashion as possible. In order to minimize the loss of HCl, the large volume of melt was added to the minute volume of water. Most of the HCl formed during the initial precipitate formation may be expected to remain in the melt.

Integrated intensities of peaks B and C as functions of composition were obtained, and the equilibrium between the two oxide species was modeled. The melt composition was corrected for the addition of $EtAlCl_2$ by assuming that $EtAlCl_2$ behaves in the same way as $AlCl_3$ (eq 1). The density of the melt at 90 °C was calculated[15] and used to calculate the concentration of water added

---

(15) Fannin, A. A.; Floreani, D. A.; King, L. A.; Landers, J. S.; Piersma, B. J.; Stech, D. J.; Vaughn, R. L.; Wilkes, J. S.; Williams, J. S. *J. Phys. Chem.* **1984**, *88*, 2614.

Table IV. Equilibria and Equilibrium Constants for Oxide Species

	equilibrium			
model	species B		species C	K (SD, G)
I	$Al_2OCl_5^- + Al_2Cl_7^-$	$\rightleftarrows$	$Al_3OCl_8^- + AlCl_4^-$	4.32 (0.88, 0.42)
II	$Al_3O_2Cl_6^- + 2Al_2Cl_7^-$	$\rightleftarrows$	$2Al_3OCl_8^- + AlCl_4^-$	0.227 (0.065, 0.83)
III	$2Al_2OCl_5^-$	$\rightleftarrows$	$Al_3O_2Cl_6^- + AlCl_4^-$	277.4 (276.3, 9.92)
IV	$AlOCl_2^- + 2Al_2Cl_7^-$	$\rightleftarrows$	$Al_3OCl_8^- + 2AlCl_4^-$	9.39 (6.08, 4.20)
V	$2Al_2OCl_5^- + Al_2Cl_7^-$	$\rightleftarrows$	$Al_4O_2Cl_9^- + 2AlCl_4^-$	408.9 (180.2, 1.94)
VI	$Al_4O_2Cl_9^- + Al_2Cl_7^-$	$\rightleftarrows$	$2Al_3OCl_8^-$	0.126 (0.073, 3.36)

present in the melt as well as the concentrations of $AlCl_4^-$ and $Al_2Cl_7^-$ present at 90 °C in the melt prior to the addition of oxide. The concentration of each species was calculated by multiplying the experimentally determined integrated intensity of each species, divided by the sum of the integrated intensities of the two peaks, by the total water concentration for each composition. For example, the concentration of species B, corresponding to NMR peak B, is

$$[B] = [H_2O](I_B/(I_B + I_C)) \tag{3}$$

where I_B and I_C are the integrated intensities of peaks B and C.

A BASIC program was written to calculate equilibrium constants for various stoichiometric models. The calculation was carried out with use of (a) the concentrations of the oxide species, taking into account the fact that the integrated intensity data must be divided by the number of oxides present in a given species to yield the actual species concentration, and (b) values for $[AlCl_4^-]$ and $[Al_2Cl_7^-]$ corrected for the creation of the former and removal of the latter in forming the oxide species.

If we represent the oxide species corresponding to NMR peaks B and C as species B, $Al_{xb}O_{yb}Cl_{zb}$, and species C, $Al_{xc}O_{yc}Cl_{zc}$, then, for the reaction

$$yc\text{B} + a_7Al_2Cl_7^- = yb\text{C} + a_4AlCl_4^- \tag{4}$$

the stoichiometric coefficients for the overall reaction are

$$a_7 = (4xc - zc)yb - (4xb - zb)yc \tag{5a}$$

and

$$a_4 = (7xc - 2zc)yb - (7xb - 2zb)yc \tag{5b}$$

The original $AlCl_4^-$ and $Al_2Cl_7^-$ concentrations are corrected for the formation of a species $Al_xO_yCl_z$ of known concentration, C, by the following equations:

$$[AlCl_4^-] = [AlCl_4^-]^\circ + \sum_{i=b,c} (7x - 2z)C_i/y \tag{6a}$$

$$[Al_2Cl_7^-] = [Al_2Cl_7^-]^\circ - \sum_{i=b,c} (4x - z)C_i/y \tag{6b}$$

The equilibrium constant K is

$$K = ([C]^{yb}[AlCl_4^-]^{a_4})/([B]^{yc}[Al_2Cl_7^-]^{a_7}) \tag{7}$$

An equilibrium constant can be independently calculated for each melt composition.

As a test of the goodness of fit of a given model, the quantity $G = \sum_n((K(n)/K') - 1)^2$ was calculated. This quantity is the sum of squares of the normalized deviations of the individual $K(n)$ values from the mean K'.

The calculations outlined above are detailed in Appendix I.

Several possible equilibria and their associated values of K', the standard deviation about the mean, denoted in the table as SD, and calculated values of G are listed in Table IV. Most of the models clearly do not fit well. K values for different compositions are not even all of the same order of magnitude for some models. Two pairs of oxychloroaluminate species fit the data reasonably well (models I and II). Structures of species with the stoichiometry indicated by these models are shown in Figure 6.

In addition to the finding that these equilibria fit the experimental data fairly well, they are satisfactory by several other criteria. Species B, which is favorable as the melt is made less acidic, has fewer chlorine atoms in the position two bonds away with respect to the oxygen than species C for both models I and II. Thus, the expected direction of inductive effects on the ^{17}O shifts for species B and C is in accord with the observed chemical shifts for the respective species. The structure shown for the dimeric species, $Al_3O_2Cl_6^-$, has the oxygens in symmetrically disposed sites, as required.[6] All species involved in the two best models appear among the species detected by mass spectroscopy.

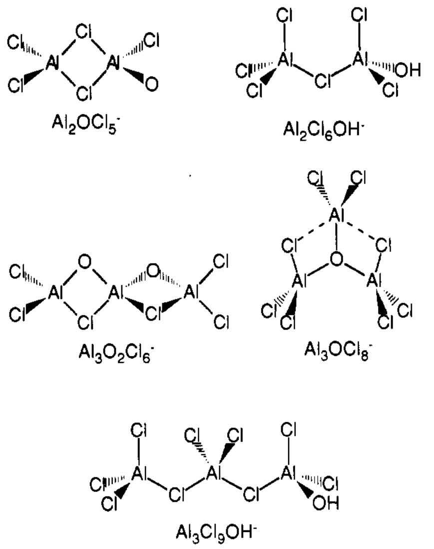

Figure 6. Species diagrams.

For nuclei with spin $>^1/_2$, relaxation is determined by the motional modulation of the nuclear electric quadrupole moment. The main factors determining the line width, assuming the extreme narrowing limit is achieved, are the rate of rotational motion, described by the rotational reorientational correlation time that varies linearly with viscosity, the size of the rotating species, and the distribution of electron density about the nucleus, determined by the site symmetry. Since they are present in the same medium and are not grossly different in size, the rotational correlation times should be the same for all species. The site symmetry of either of the possible B species is lower than that of species C, in accord with the observed line widths.

In spite of the somewhat poorer statistics, model II is preferable on several qualitative counts. First, the mass spectral peaks observed indicate two different classes of oxide present in acidic melts, those containing one and two oxygen atoms per complex. One can consider the various observed species to be solvated forms of the "root" species AlO^+ and AlO_2^-. The species detected by mass spectroscopy can all be derived from the root species via transfers of HCl and $AlCl_3$ units. The latter type of interconversions may be comparable to processes occurring in the plasma above the sample in a mass spectral experiment since HCl and $AlCl_3$ probably both evaporate from the melt droplet. The two species involved in model II represent the two classes of species derived from the two root species, while only one class is represented by the species of model I.

Second, these species are consistent with the results obtained by Berg et al.[4] and Zachariassen et al.,[5] who used cryoscopy and potentiometry to obtain information on oxide speciation in the higher melting $NaCl/AlCl_3$ system. The dimeric species postulated in model II is favored as the melt approaches the neutral point from the acidic side, in accord with the findings of refs 4 and 5. Though the melt acidity is probably different, the chemical nature of the $NaCl/AlCl_3$ melt is similar to that of the lower melting organic chloride/$AlCl_3$ melts. Thus, it is quite reasonable to expect similar types of species, perhaps solvated slightly differently (i.e., with additional $AlCl_4^-$ moieties added on).

In Appendix II, we describe the modeling of ^{17}O data for proton-containing water solutions in acidic melts. In this model, we assume that protons are present in the acidic melt as HCl, an

---

(16) Klemperer, W. G.; Shum, W. J. *J. Am. Chem. Soc.* **1978**, *100*, 4891.

(17) Filowitz, M.; Ho, R. K. C.; Klemperer, W. G.; Shum, W. J. *Inorg. Chem.* **1979**, *18*, 93.

Table V. Equilibrium Constants from Modeling All Species Present[a]

species A	species B	K_{ab} (SD, G)	K_{bc} (SD, G)
$Al_2Cl_6OH^-$	$Al_3O_2Cl_6^-$	0.89 (±0.77, 7.1)	0.27 (±0.048, 0.38)
$Al_2Cl_6OH^-$	$Al_2OCl_5^-$	0.10 (±0.063, 0.05)	4.32 (± 1.14, 0.83)
$Al_3Cl_9OH^-$	$Al_3O_2Cl_6^-$	0.10 (±0.065, 0.05)	0.28 (±0.047, 0.34)
$Al_3Cl_9OH^-$	$Al_2OCl_5^-$	0.034 (±0.014, 0.002)	4.40 (±1.14, 0.81)
$AlCl_3OH^-$	$Al_3O_2Cl_6^-$	15 (±21, 5334)	0.26 (±0.05, 0.45)
$AlCl_3OH^-$	$Al_2OCl_5^-$	0.38 (±0.36, 1.53)	4.24 (±1.13, 0.86)
$Al_3Cl_{10}OH^{2-}$	$Al_3O_2Cl_6^-$	9.22 (±9.73, 1136)	0.27 (±0.047, 0.39)
$Al_3Cl_{10}OH^{2-}$	$Al_2OCl_5^-$	0.32 (±0.23, 0.64)	4.30 (±1.13, 0.83)

[a] Species C is assumed to be $Al_3OCl_8^-$.

assumption supported by our previous work on Im^2HCl_2 chemical shift measurements.[12] Equations similar to those given above can be derived for the case in which all three species are present. In the following discussion, species A has the formula $Al_{xa}Cl_{za}(OH)_{ya}$ and the appendage "*ab*" refers to equilibrium constants and stoichiometric coefficients for the equilibrium

$$ybA + a_{7ab}Al_2Cl_7^- = yaB + a_{4ab}AlCl_4^- + yaybHCl \quad (8)$$

with

$$a_{7ab} = ya(4xb - zb) - yb(ya + 4xa - za) \quad (9)$$

and

$$a_{4ab} = ya(7xb - 2zb) - yb(2ya + 7xa - 2za) \quad (10)$$

Equations 4–7 still obtain with appropriate subscripts "*bc*" on the stoichiometric coefficients and equilibrium constants and with the terms $[+(ya + 4xa - za)C_a/ya]$ and $[-(2(ya - za) + 7xa)C_a/ya]$ added to the ends of eqs 6a and 6b, respectively.

If we accept models I and II shown above as the most satisfactory descriptions of speciation in the absence of protons, then modeling all three species can give us the identity of species A and may possibly discriminate between the two possible species B. The results of modeling all three species are summarized in Table V. From these results, we see that the species $Al_2Cl_6OH^-$ and $Al_3Cl_9OH^-$ fit the data reasonably well. It is interesting, and gratifying, to note that the equilibrium constants derived from this data set for the equilibrium constant between species B and C are essentially the same as those derived from the oxide-only data. The two hydroxychloroaluminate species observed correspond to replacement of $AlCl_3$ with HCl and direct substitution of HCl onto the $Al_3OCl_8^-$ species. HCl can be thought of as chemically analogous to $AlCl_3$, the former being a Brønsted rather than a Lewis acid. Thus, in addition to protonation, replacement of an $AlCl_3$ moiety in species C by HCl to form species A is a reasonable assumption. If an $AlCl_3$ unit is replaced by HCl in $Al_3OCl_8^-$, for example, the species $Al_2Cl_6OH^-$ is created, as indicated by the following reaction:

$$Al_3OCl_8^- + HCl + AlCl_4^- = Al_2Cl_6OH^- + Al_2Cl_7^- \quad (11)$$

The replacement of $AlCl_3$ by HCl also is in better agreement with the observed slow exchange rate between acidic melt species (see below). Of the two species, only $Al_2Cl_6OH^-$ is observed by SIMS. However, $Al_3Cl_9OH^-$ fits the data reported here with somewhat better statistics.

Reaction 11 accords well with the NMR data shown in our previous publication;[6] as the melt is made more acidic, the equilibrium will shift to the left, in accord with the observed trend in integrated intensities. By contrast, the addition of HCl to $Al_3OCl_8^-$ to form $Al_3Cl_9OH^-$ should be approximately independent of melt composition. (The "approximately" could be due to the change of the HCl activity coefficient to higher values as the melt is made more acidic.)[18] However, there is another equilibrium involved, and thus naive consideration of a single equilibrium is not adequate justification for ruling out $Al_3Cl_9OH^-$ as a plausible species A. Also, if species A is $Al_2Cl_6OH^-$, the upfield chemical shift observed for species A relative to species C would be expected since species A has fewer chlorides in the β-position to the oxygen. Protonation itself leads to an upfield chemical shift. Thus, we favor the identification of species A with the complex ion $Al_2Cl_6OH^-$.

Table VI. Concentrations of Various Species Involved in Oxide Equilibrium[a]

melt compn, mole ratio of $AlCl_3$ to ImCl	$[AlCl_4^-]$	$[Al_2Cl_7^-]$	$[O^{2-}]_T$	$[O^{2-}]_B$	$[O^{2-}]_C$
1.20	3.30	0.82	48.14	26.10	22.04
1.25	3.02	1.02	48.15	19.36	28.81
1.30	2.73	1.17	48.18	19.26	28.93
1.32	2.71	1.25	48.19	17.74	30.45
1.40	2.33	1.53	48.23	15.78	32.45
1.41	2.27	1.57	48.23	16.52	31.72
1.47	2.01	1.76	48.26	11.37	36.86
1.50	1.85	1.88	48.27	10.22	38.06
1.54	1.72	1.97	48.29	7.71	40.58
1.60	1.46	2.16	48.32	6.09	42.22

[a] $[AlCl_4^-]$ and $[Al_2Cl_7^-]$ are in molar units; $[O^{2-}]_T$, $[O^{2-}]_B$, are $[O^{2-}]_C$ are in millimolar units.

A hypothesis concerning the species present in basic melts may be deduced by considering the NMR data for the various species, the chemical nature of the acidic and basic melts, the inductive effects of electronegative groups near the oxygen, and the effect of protonation on the chemical shift of an oxygen. In acidic melts, the chemical shift of oxygen is about 43 ppm greater in environment C than that in environment A, which is protonated and has two less chlorine atoms two bonds away, according to the model presented above. The shift between environments C and B is 18 ppm, and site B has three fewer electronegative atoms two bonds away. If we consider the oxychloroaluminate species present in the basic melt, species D, to be $Al_2OCl_5^-$, the only oxygen-containing species observed in mass spectral studies of basic melts, then a shift of 23 ppm between peaks C (at ca. 92 ppm) and D (at ca. 69 ppm) is observed. The number of electronegative atoms two bonds away is 3 fewer for site D than for site C. Comparing B (ca. 74 ppm) and D, for which approximately similar chemical shifts are observed, the oxygens in these two species are likely to be in fairly similar chemical environments. A species with this stoichiometry is shown in Figure 6. Note the similarity in structure between this species and $Al_3O_2Cl_6^-$.

The hydroxychloroaluminate species present in the basic melt, species E, has a chemical shift roughly 45 ppm upfield of species D. The magnitude of this difference is roughly the same as that between species C and A. Thus, we might expect a difference of two chlorine atoms two bonds away in addition to protonation. Two species that fit this description are $AlCl_3OH^-$ and $Al_2Cl_6OH^-$, with the –OH terminal instead of bridging. The latter species appears more likely since loss of HCl from this species directly produces $Al_2OCl_5^-$, the only oxygen-containing ion reported from SIMS experiments on a basic melt. Since there is apparently less $AlCl_3$ evaporated from a basic melt during the SIMS experiment, the formation of $Al_2OCl_5^-$ from $AlCl_3OH^-$ is less likely. The simple protonation/deprotonation reaction is expected to be fast, as observed. The implied ^{17}O-exchange rates are much faster in basic than in acidic melts. This is reasonable, since we note that the rate of $AlCl_3$ transfer between $AlCl_4^-$ and $Al_2Cl_7^-$ in the acidic melts is slow. That is, the solvent self-exchange

$$*AlCl_4^- + Al_2Cl_7^- \rightarrow *AlCl_4AlCl_3^- + AlCl_4^- \quad (12)$$

has been shown to be surprisingly slow.[19,20]

It is clear from the stoichiometry and structures presented that the speciation proposed is consistent with the expected complexing properties of the melt. In the species characteristic of acidic melts, the oxygen atoms are generally surrounded by more aluminum atoms than in basic melts. The arguments presented above, though speculative, are based on the available experimental evidence and

---

[18] Smith, G. P.; Dworkin, A.; Pagni, R. M.; Zingg, S. P. *J. Am. Chem. Soc.* **1989**, *111*, 5075.

[19] Gray, J. L.; Maciel, G. *J. Am. Chem. Soc.* **1981**, *103*, 7147.

[20] Matsumato, T.; Ichikawa, K. *J. Am. Chem. Soc.* **1984**, *106*, 4136.

Table VII. Concentration of Species Involved in Equilibria Modeled[a]

melt compn, mole ratio of $AlCl_3$ to ImCl	$[AlCl_4^-]$	$[Al_2Cl_7^-]$	[HCl]	$[O^{2-}]_A$	$[O^{2-}]_B$	$[O^{2-}]_C$
1.44	2.07	1.74	0.065	0.015	0.013	0.041
1.38	2.31	1.55	0.074	0.012	0.017	0.040
1.37	2.38	1.51	0.076	0.012	0.018	0.040
1.26	2.94	1.10	0.093	0.019	0.026	0.027
1.31	2.66	1.30	0.085	0.012	0.025	0.034
1.24	3.06	1.01	0.097	0.011	0.032	0.049
1.20	3.24	0.88	0.102	0.036	0.020	0.017
1.20	3.21	0.91	0.070	0.018	0.032	0.024
1.20	3.18	0.93	0.050	0.008	0.038	0.028
1.20	3.16	0.95	0.028	0.005	0.042	0.027
1.52	1.71	2.00	0.053	0.014	0.007	0.046
1.52	1.68	2.03	0.020	0.006	0.010	0.051
1.52	1.66	2.05	0.006	0.002	0.011	0.055

[a] All concentrations are in molar units.

represent a logically consistent and complete model of oxide chemistry in the chloroaluminate melts. This model can be summarized by the following set of reactions. (Note that reactions 14 and 14a are *not* those for which equilibrium constants were calculated; since we have a clear idea of what species C is, we have, for the sake of convenience, written here equilibrium *ac* instead of *ab*.)

acidic melts

$$Al_3O_2Cl_6^- + 2Al_2Cl_7^- \rightleftarrows 2Al_3OCl_8^- + AlCl_4^- \quad (13)$$

or

$$Al_2OCl_5^- + Al_2Cl_7^- \rightleftarrows Al_3OCl_8^- + AlCl_4^- \quad (13a)$$

$$Al_3OCl_8^- + HCl + AlCl_4^- \rightleftarrows Al_2Cl_6OH^- + Al_2Cl_7^- \quad (14)$$

or

$$Al_3OCl_8^- + HCl \rightleftarrows Al_3Cl_9OH^- \quad (14a)$$

basic melts

$$Al_2OCl_5^- + HCl \rightleftarrows Al_2Cl_6OH^- \quad (15)$$

Acknowledgment. This work was supported in part by the Air Force Office of Scientific Research.

Appendix I. Modeling of ^{17}O NMR Data for Oxide Species in Acidic Melts

The modeling of the oxide speciation in acidic melts based on the composition-dependent ^{17}O NMR data is outlined in this appendix.

All solutions were prepared in the following manner. Approximately 50 mM ^{17}O-labeled water was added to melts of composition MC = 1.16 and 1.63. These two solutions were then treated with a near-stoichiometric amount of $EtAlCl_2$. The treated solutions are hereafter referred to as stock solutions. The compositions of these melts were corrected for the addition of $EtAlCl_2$ by treating 1 mol of $EtAlCl_2$ as 1 mol of $AlCl_3$ added to the melt. Slightly less $EtAlCl_2$ than twice the molar amount of water added was used to avoid overtitration. The additional peaks observed due to overtitration in previous experiments were not observed in this case, and thus the perturbation of the equilibrium studied due to the presence of the species corresponding to the peaks typical of an overtitrated solution was judged to be minimal. Solutions of oxide in melts of intermediate composition were prepared by mixing the two stock solutions of oxide in melts in various proportions. The composition was then calculated as the weighted average of the corrected compositions of the stock solutions.

In Table III, the melt composition and integrated intensities and line widths of peaks B and C are given for the solutions of oxide in melts used in the modeling. From the melt composition and the melt density at 90 °C, the concentration of $AlCl_4^-$, $Al_2Cl_7^-$, and oxide can be calculated for the experimental conditions employed. The density of the melt at 90 °C was estimated from the data presented by Fannin et al.[15] These concentrations are given in Table VI, together with the concentrations of species B and C calculated from the product of the total oxide concentration with the fraction of the total integrated intensity observed for each peak in the ^{17}O NMR spectrum.

With the above concentrations as input, the equilibria were modeled by "guessing" at pairs of species to represent B and C. The concentration of the species and the stoichiometry of the hypothetical complexes B and C were used to correct $[AlCl_4^-]$ and $[Al_2Cl_7^-]$ for the formation of species B and C. The complex stoichiometries were also used to calculate the reaction stoichiometry. For a given pair of species, an equilibrium constant can be calculated. The stoichiometric relationships and equilibrium constant expression used in the calculations are given in Table IV. The modeling above was carried out with a computer program written in BASIC.

Appendix II. Modeling of ^{17}O NMR Data for All Species Present

The modeling of the ^{17}O NMR data to determine oxide and hydroxide speciation in acidic melts is discussed in this appendix.

Solutions were prepared in a manner similar to that described in Appendix I, with stock solutions of MC = 1.20 and 1.53. In this case, however, the protons were removed from samples of the stock solutions via several additions of $EtAlCl_2$ and the NMR spectra were determined after each addition. This enabled us to estimate the initial concentrations of protons present in each of the stock solutions. Compositions of the stock solutions were corrected for the formation of HCl upon addition of water to the melt, and the melt compositions and proton concentrations of each solution of intermediate composition were calculated as weighted averages of the respective quantities characteristic of the stock solutions. Concentrations of other species present were calculated as outlined in Appendix I. The concentrations of each of the species present as a function of melt composition are given in Table VII. The modeling of the two equilibria was performed as indicated in Appendix I, with the modification that three species were guessed and appropriate changes in the program used for the calculations.